

Three-Dimensional Simulations of the Deflagration Phase of the Gravitationally Confined Detonation Model of Type Ia Supernovae

G. C. Jordan IV,^{1,2} R. T. Fisher,^{1,2} D. M. Townsley,^{3,2} A. C. Calder,^{1,2,7} C. Graziani,^{1,2}
S. Asida,⁴ D. Q. Lamb,^{1,2,5} and J. W. Truran,^{1,2,5,6}

ABSTRACT

We report the results of a series of three-dimensional simulations of the gravitationally confined detonation mechanism for Type Ia supernovae. In this mechanism, ignition occurs at one or several off-center points, resulting in a burning bubble of hot ash that rises rapidly, breaks through the surface of the star, and collides at a point opposite breakout on the stellar surface. We find that detonation conditions are robustly reached in our three-dimensional simulations for a range of initial conditions and resolutions. These conditions are achieved as the result of an inwardly-directed jet that is produced by the compression of unburnt surface material when the surface flow collides with itself. A high-velocity outwardly-directed jet is also produced. Recent observations of Type Ia supernovae imply properties that are consistent with those expected from these 3D simulations of the GCD model.

Subject headings: hydrodynamics – nuclear reactions, nucleosynthesis, abundances – supernovae: general – white dwarfs

¹Center for Astrophysical Thermonuclear Flashes, The University of Chicago, Chicago, IL 60637.

²Department of Astronomy and Astrophysics, The University of Chicago, Chicago, IL 60637.

³Joint Institute for Nuclear Astrophysics, The University of Chicago, Chicago, IL 60637.

⁴Racah Institute of Physics, Hebrew University, Jerusalem 91904, Israel.

⁵Enrico Fermi Institute, The University of Chicago, Chicago, IL 60637.

⁶Argonne National Laboratory, Argonne, IL 60439.

⁷ Now at Department of Physics and Astronomy, SUNY Stony Brook, Stony Brook, NY 11794-3800.

1. Introduction

Type Ia supernovae have received increased interest because of their importance as “standard candles” for cosmology. Observations using Type Ia supernovae as standard candles have revealed that the expansion rate of the universe is accelerating and have led to the discovery of “dark energy” (Riess et al. 1998; Perlmutter et al. 1998). However, the way in which Type Ia supernovae explode is not fully understood. The current leading paradigms for the explosion mechanism are (1) pure deflagration (Reinecke et al. 2002; Gamezo et al. 2003; Röpke & Hillebrandt 2005), (2) deflagration to detonation transition (DDT) (Khokhlov 1991; Gamezo, Khokhlov & Oran 2004; Gamezo et al. 2005), (3) pulsational detonation (PD) (Khokhlov 1991), and (4) gravitationally confined detonation (GCD) (Plewa, Calder, & Lamb 2004; Livne et al. 2005; Plewa 2007; Townsley et al. 2007). There is increasing evidence that in order to reproduce observed isotopic abundances, a detonation must follow a deflagration (Höflich et al. 2002; Badenes et al. 2006; Wang et al. 2006, 2007; Gerardy et al. 2007), as is posited in the last three explosive models. However, a fundamental question has been how the transition to a detonation occurs in a white dwarf star [see, e.g., Niemeyer (1999)]. While the DDT, PD, and GCD paradigms all incorporate a detonation, all existing DDT simulations invoke the transition to a detonation in an ad-hoc fashion, and the PD mechanism remains largely unexplored by detailed simulations. Thus, to date, the GCD mechanism is the only proposed mechanism for which the detonation has been demonstrated to arise naturally.

Extensive 2-D cylindrical simulations have shown that detonation conditions are robustly reached in the GCD model for a range of initial conditions (Plewa, Calder, & Lamb 2004; Plewa 2007; Röpke, Woosley, & Hillebrandt 2007; Townsley et al. 2007). However, the achievement of detonation conditions has not been demonstrated in three dimensions (3-D) [see, e.g., Röpke, Woosley, & Hillebrandt (2007)]. Hence, a major question that we address in this Letter is whether it is possible to achieve detonation conditions in a fully 3-D simulation of the GCD scenario.

In this Letter, we report the results of seven 3-D simulations of the GCD mechanism for a range of initial conditions. We find that the conditions for detonation are robustly achieved in all of the simulations.

2. Simulations

We perform our 3-D simulations using FLASH 3.0, an adaptive-mesh hydrodynamics code (Fryxell et al. 2000; Calder et al. 2002). The nuclear flame is followed using a new

version (Asida et al. 2007) of the advection, diffusion, reaction (ADR) flame model that we used previously (Khokhlov 1995; Vladimirova, Weirs, & Ryzhik 2006; Calder et al. 2004; Plewa, Calder, & Lamb 2004; Plewa 2007). The new prescription uses the Kolmogorov-Petrovski-Piskunov (KPP) form of the reaction term in which this term is slightly truncated. This new version is numerically quieter, more stable, and exhibits far smaller curvature effects (Asida et al. 2007). We also use a new, acoustically-quiet version (Townsley et al. 2007) of the nuclear energy release method described in Calder et al. (2007) which accounts more accurately for the nuclear energy released in the flame and in the evolution of nuclear statistical equilibrium (NSE) as conditions change within the bubble of hot ash.

The general simulation setup is the 3-D equivalent of that described in Townsley et al. (2007). In particular, we assume that ignition occurs at a single point near the center of the star and follow the simulations through bubble breakout until maximum temperature and density have been reached in the collision region. In order to simplify the simulations, we begin with no velocity field in the star, even though the core is convective and therefore a nonzero velocity field is expected (Woosley, Wunsch, & Kuhlen 2004; Wunsch & Woosley 2004). (We will investigate ignition at multiple points and the effects of convective motions in the core of the star in future papers.) The initial model is a $1.38 M_{\odot}$ WD with a uniform composition of equal parts by mass of ^{12}C and ^{16}O . This model has a central density of $2.2 \times 10^9 \text{ g cm}^{-3}$, a uniform temperature of $4 \times 10^7 \text{ K}$, and a radius of approximately 2,000 km.

In the scenario we investigate, a single, small region ignites near the center of the white dwarf, grows spherically, and initially rises slowly due to its small size and proximity to the center of the star. We choose to model the ignition region as a spherical bubble of hot ash initially at rest characterized by an initial radius, r_{bubble} , and initial distance, r_{offset} , from the center of the star along the z-axis. Physical self-consistency then imposes a constraint on the combination of r_{bubble} and r_{offset} . Specifically, r_{bubble} must satisfy $r_{\text{bubble}} \lesssim \lambda_c \equiv 2\pi s^2/Ag$ (where s is the laminar flame speed, $A = (\rho_{\text{fuel}} - \rho_{\text{ash}})/(\rho_{\text{fuel}} + \rho_{\text{ash}})$ is the Atwood number, and g is the acceleration of gravity at r_{offset}). Otherwise, the initial bubble is immediately highly unstable to the growth of Rayleigh-Taylor modes (Fisher et al. 2007), which is inconsistent with the assumption of a spherical initial bubble.

The edge of the burned region is formed by a smooth transition from fuel to ash within ~ 4 zones in width [see Townsley et al. (2007) for more details]. The adaptive mesh refinement has been chosen to capture the relevant physical features of the burning and the flow at reasonable computation expense. The general prescription for refinement is similar to that described in Townsley et al. (2007), except that we maximally resolve a truncated cone encompassing the region where the flow of hot bubble material over the surface of the star

collides with itself.

We label the seven 3-D simulations of the deflagration phase of the GCD mechanism we performed by r_{bubble} , r_{offset} , and the finest resolution in the simulation. For example, the 3-D simulation in which $r_{\text{bubble}} = 16$ km, $r_{\text{offset}} = 20$ km, and the finest resolution is 8 km is denoted by 16b20o8r. The other six simulations we performed are 18b42o6r, 16b40o8r, 16b100o8r, 25b100o6r, 25b100o8r, and 50b100o8r.

3. Results

Our 3-D simulations progress similarly to previous 2-D GCD simulations (Plewa, Calder, & Lamb 2004; Plewa 2007; Townsley et al. 2007) and pass through several stages of evolution. First, the single ignition bubble initially grows at a rate dictated by the laminar flame speed. At $\sim 0.2 - 0.3$ sec of simulation time the radius r_{bubble} of the bubble exceeds λ_c , the minimum wavelength for the Rayleigh-Taylor instability on a propagating flame front (Khokhlov 1995; Zhang et al. 2007), the top surface of the bubble develops a bulge, and the bubble quickly evolves into a mushroom-like shape (Calder et al. 2004; Plewa, Calder, & Lamb 2004; Vladimirova, Weirs, & Ryzhik 2006; Plewa 2007; Townsley et al. 2007). Subsequently, the shape of the bubble becomes ever more complex as the critical wavelength λ_c becomes smaller (as the bubble rises through the changing conditions of the star) and additional generations of smaller features appear as a result of the Rayleigh-Taylor instability. During this time, the bubble rises rapidly, and breaks through the stellar surface at $\sim 0.8 - 1.2$ sec. The hot bubble material then spreads rapidly over the surface of the star, pushing unburned material ahead of it. At $\sim 1.8 - 2.2$ sec, this flow collides with itself at the opposite point on the stellar surface from the place where the bubble broke out, compresses the unburnt surface layers there, and initiates a detonation (Plewa, Calder, & Lamb 2004; Plewa 2007; Townsley et al. 2007).

The unburnt surface material in the initial collision region reaches $T > 3 \times 10^9$ K but densities of only $\rho \sim 10^5 - 10^6$ g cm $^{-3}$, which are insufficient to detonate (Niemeyer & Woosley 1997). This compression, however, produces inwardly- and outwardly- directed jets. The outward jet ejects material at velocities $v_{\text{jet}} \sim 40,000$ km s $^{-1}$. The inward jet impacts the stellar surface, stalls, and spreads a bit. This sequence of events compresses the hot ($T > 3 \times 10^9$ K) material in the jet to densities $\rho > 1 \times 10^7$ g cm $^{-3}$, and in some cases even $\rho > 2 \times 10^7$ g cm $^{-3}$, as shown in Figure 1. These conditions exceed conservative conditions for detonation (Niemeyer & Woosley 1997; Röpke, Woosley, & Hillebrandt 2007). Thus, it is the kinetic energy originating from breakout imparted to the unburnt surface layers of the star by the inwardly-moving jet generated by collision of the surface flows that causes the

unburnt material to achieve the conditions for detonation [see also Townsley et al. (2007)]. Figure 1, which shows the temperature and density in the collision region, illustrates this process.

We find that the unburnt material in the surface layers of the star reaches temperatures $T > 2 \times 10^9$ K and densities $\rho > 1 \times 10^7$ g cm $^{-3}$ in all seven 3-D simulations we performed, as illustrated in Figure 2. The values of T and ρ that are reached closely match those in our 2-D cylindrical simulations for the same resolution and initial conditions (Townsley et al. 2007). Thus the results of our 2-D cylindrical simulations are a good guide to the results of our 3-D simulations for the range of offset distances and resolutions that we have explored so far.

In order to test the robustness of the GCD mechanism, we ran additional simulations with the same resolution and initial conditions as the 25b100o8r simulation. In these simulations, we deresolved a truncated cone encompassing the collision region. The truncated cone extended from 1500 km to 3000 km in radius and had finest resolutions of 16 km, 32 km, and 64 km. In all cases, the simulations reached the above conservative conditions for detonation. We conclude that the GCD mechanism robustly achieves the conditions necessary for detonation.

4. Discussion

Röpke, Woosley, & Hillebrandt (2007) have recently conducted an extensive set of 2-D cylindrical simulations and a few 3-D simulations of the GCD mechanism. They find that the conditions for detonation are reached for a number of their 2-D cylindrical simulations spanning a range of initial offset distances. They report, however, that their 3-D simulations did not reach conditions for detonation. In contrast, the seven 3-D simulations we present here all exceed conservative conditions for detonation ($T > 2 \times 10^9$ K, $\rho > 1 \times 10^7$ gm cm $^{-3}$).

In Figure 3, we plot T_{\max} , the maximum temperature attained in the collision region versus E_{nuc} , the nuclear energy release, for all of the 3-D simulations we present here and our previous 2-D simulations (Townsley et al. 2007), and for the 2-D and 3-D simulations of Röpke, Woosley, & Hillebrandt (2007). This figure shows that there is a relation between T_{\max} in the collision region and E_{nuc} . Such a relation is expected in the GCD mechanism to the degree that larger values of E_{nuc} produce more pre-expansion of the star, and therefore less kinetic energy in the flow of hot bubble material over the stellar surface, leading to lower values of T in the collision region. The results from our 2-D cylindrical and 3-D simulations agree with each other and satisfy this relation, and also agree with the results of Roepke et

al.’s 2-D cylindrical simulations for single bubbles, perturbed bubbles, and teardrop-shaped bubbles (both one-sided and two-sided). However, their 3-D simulations for these three initial bubble configurations do not satisfy this relation, and thus disagree with both the results of their own 2-D cylindrical simulations, and the results of our 2-D cylindrical and 3-D simulations.

In an effort to understand the origin of this disagreement, we have carried out 6-km and 8-km resolution simulations for exactly the same initial conditions as were used for one of the two Röpke, Woosley, & Hillebrandt (2007) 3-D simulations: an initial bubble radius of 25 km and an offset distance of 100 km (see above). [We did not simulate the other initial conditions for which Röpke, Woosley, & Hillebrandt (2007) did a 3-D simulation (i.e., an initial bubble radius of 25 km and an offset distance of 200 km) because these initial conditions lie far above the $r_{\text{bubble}} = \lambda_c$ curve, and are therefore far from being physically self-consistent (Fisher et al. 2007).] Additionally, we carried out an 8-km resolution simulation with an initial bubble radius $r_{\text{bubble}} = 50$ km and an offset distance $r_{\text{offset}} = 100$ km, in an attempt to understand the failure of Röpke et al.’s 3-D multiple-bubble simulations to achieve the conditions for detonation. In all cases, the simulations reached conservative conditions for detonation. These results provide additional evidence of the ability of the GCD mechanism to robustly produce the conditions for detonation, but leave unanswered the question of why the Röpke, Woosley, & Hillebrandt (2007) 3-D simulations do not follow the $T_{\text{max}}-E_{\text{nuc}}$ relation and do not reach the conditions for detonation.

We find that our 3-D simulations exhibit a correlation between E_{nuc} and initial offset distance, confirming the correlation seen in our 2-D cylindrical simulations (Townsley et al. 2007). We also find that the simulation in which the radius of the initial bubble $r_{\text{bubble}} = 50$ km [which greatly exceeded λ_c , and therefore is not expected to exhibit self-similar behavior, as do bubbles for which $r_{\text{bubble}} < \lambda_c$ (Vladimirova, Weirs, & Ryzhik 2006; Fisher et al. 2007)] had much larger values of E_{nuc} , but still reached the above conservative conditions for detonation.

Simulations that start with large bubbles at large radii may crudely mock up what happens if ignition occurs simultaneously at a few off-centered points near the center of the star, since in this case the bubbles will grow but hardly rise until they merge, at which point the drag force becomes less and the entity formed by the merger will begin to rise rapidly. Thus the 50b100o8r simulation suggests a plausible way in which the GCD mechanism can produce much more pre-expansion, and therefore much less nickel, yet robustly detonate – i.e., one way in which the GCD mechanism might account for less luminous Type Ia supernovae.

In the GCD mechanism, the deflagration phase causes the star to expand prior to

the initiation of a detonation, yet leaves the majority of the star unburnt and undisturbed (Plewa, Calder, & Lamb 2004; Plewa 2007; Townsley et al. 2007). The subsequent detonation phase therefore mimics earlier 1-D simulations (Nomoto, Thielemann, & Yokoi 1984), which match the smooth, stratified composition in the core of the star that is inferred from spectroscopic observations much better than do 2-D cylindrical and 3-D simulations of both the pure deflagration model [see, e.g. Höflich et al. (2002); Wang et al. (2004); Leonard et al. (2005); Badenes et al. (2006); Wang et al. (2006, 2007)], and the deflagration to detonation (DDT) model [see, e.g. Gerardy et al. (2007)]. The GCD model also produces turbulence and compositional inhomogeneities in the outermost layers of the star, which match the conditions inferred from observations of line polarization in the optical (Wang et al. 2006, 2007) and line profiles in the NIR and MIR (Gerardy et al. 2007). Thus, while the pure deflagration and DDT mechanisms predict an inhomogeneous, mixed composition in the core and a uniform composition in the outermost layers of the star, which is opposite to the situation inferred from observations, the GCD mechanism predicts a smoothly-stratified composition in the core and an inhomogeneous, mixed composition in the outermost layers of the star, in agreement with the situation inferred from these observations.

5. Conclusions

We have conducted a series of 3-D simulations of the GCD mechanism for several offset distances and resolutions. Conservative conditions for detonation are robustly achieved in all cases. We find a correlation between the central density of the star at detonation and both the offset distance and the radius of the initial bubble. These correlations offer a possible explanation for the observed variation in nickel mass in Type Ia supernovae. In addition, the uniform, homogeneous cores and the turbulent, heterogeneous composition of the outer layers of the stars at the time when the conditions for detonation are reached match the properties inferred from recent polarization and spectroscopic observations.

We thank Nathan Hearn for his software analysis tools, discussions of this work, and his invaluable assistance in preparing this paper. We thank the code group at the ASC/Flash Center, especially Anshu Dubey, Lynn Reid, Paul Rich, Dan Sheeler, and Klaus Weide, for both code development and help in running the simulations; and Brad Gallagher for visualizing the resulting data. We thank LLNL Computing for help in running our simulations on uP at LLNL and the NERSC support staff at LBNL for help in running on Bassi and Seaborg. We also acknowledge the help of Hank Childs and the VisIt team at LLNL. This work is supported in part at the University of Chicago by the U.S Department of Energy (DOE) under Contract B523820 to the ASC Alliances Center for Astrophysical Nuclear Flashes, and in

part by the National Science Foundation under Grant PHY 02-16783 for the Frontier Center “Joint Institute for Nuclear Astrophysics” (JINA). ACC acknowledges support from NSF Grant ST-0507456. JWT acknowledges support from Argonne National Laboratory, which is operated under DOE Contract No. W-31-109-ENG-38. This research used resources awarded under the INCITE program at LBNL NERSC, which is supported by the Office of Science of the U.S. Department of Energy under Contract No. DE-AC03-76SF00098.

REFERENCES

Asida, S., et al. 2007, ApJ, to be submitted

Badenes, et al. 2006, ApJ, 645, 1373

Calder, A. C., et al. 2002, ApJS, 143, 201

Calder, A. C., et al. 2004, astro-ph/0405162

Calder, A. C., et al. 2007, ApJ, 656, 313

Fisher, R., et al. 2007, ApJ, to be submitted

Fryxell, B., et al. 2000, APJS, 131, 273

Gamezo, V. N., et al. 2003, Science, 299, 77

Gamezo, V. N., Khokhlov, A. M., & Oran, E. S. 2004, Phys. Rev. Lett., 92, 211102

Gamezo, V. N., Khokhlov, A. M., & Oran, E. S. 2005, ApJ, 623, 337

Gerardy, C., et al. 2007, ApJ, submitted (astro-ph/0702117)

Höflich, P., et al. 2002, ApJ, 568, 791

Khokhlov, A. M. 1991, 2, 245, 114

Khokhlov, A. M. 1995, ApJ, 449, 695

Leonard, D C., et al. 2005, ApJ, 632, 450

Livne, E. Asida, S . M.& Höflich, P. 2005, ApJ, 632, 443

Niemeyer, J. C. 1999, ApJ, 523, L57

Niemeyer, J. C. & Woosley, S. E. 1997, ApJ, 475, 740

Nomoto, K., Thielemann, F.-K., & Yokoi, K. 1984, *ApJ*, 286, 644

Perlmutter, S., et al. 1998, Abstracts of the 19th Texas Symposium on Relativistic Astrophysics and Cosmology, held in Paris, France, Dec. 14-18, 1998. Eds.: J. Paul, T. Montmerle, and E. Aubourg (CEA Saclay)

Plewa, T. 2007, *ApJ*, 657, 942

Plewa, T., Calder, A. C., & Lamb, D. Q. 2004, *ApJ*, 612, L37

Reinecke, et al. 2002, 2, 391, 1167

Riess, A., et al. 1998, *AJ*, 116, 1009

Röpke, F., & Hillebrandt, W. 2005, 2, 431, 635

Röpke, F., Woosley, S. E., & Hillebrandt, W. 2007, *ApJ*, accepted (astro-ph/0609088).

Townsley, D., et al. 2007, *ApJ*, submitted

Vladimirova, N., Weirs, G., & Ryzhik, L. 2006, *Combust. Theory Modeling*, 10, 727

Wang, L., et al. 2004, *ApJ*, submitted (astro-ph/0409593)

Wang, L., et al. 2006, *ApJ*, 653, 490

Wang, L., et al. 2007, *Science*, 315, 212

Woosley, S. E., Wunsch, S., & Kuhlen, M. 2004, *ApJ*, 607, 921

Wunsch, S. & Woosley, S. E. 2004, *ApJ*, 616, 1102

Zhang, J., et al. 2007, *ApJ*, 656, 347

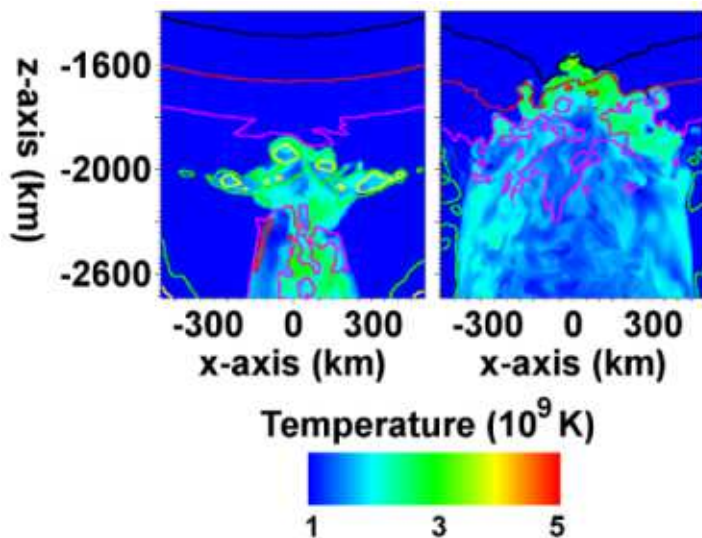


Fig. 1.— Close-up view of 2-D slices of the region near the “south pole” of the star. The slices show the inward-directed jet produced by the collision of unburnt material ahead of the hot ash from the bubble in the 25b100o6r simulation just prior to and after the density of the hot material in the jet has reached its maximum value. The color shows the temperature, ranging from 1×10^9 - 5×10^9 K and the lines are contours of density are 5×10^5 gm/cm³ (yellow), 1×10^6 (green), 5×10^6 (pink), 1×10^7 (red), and 2×10^7 gm/cm³ (black).

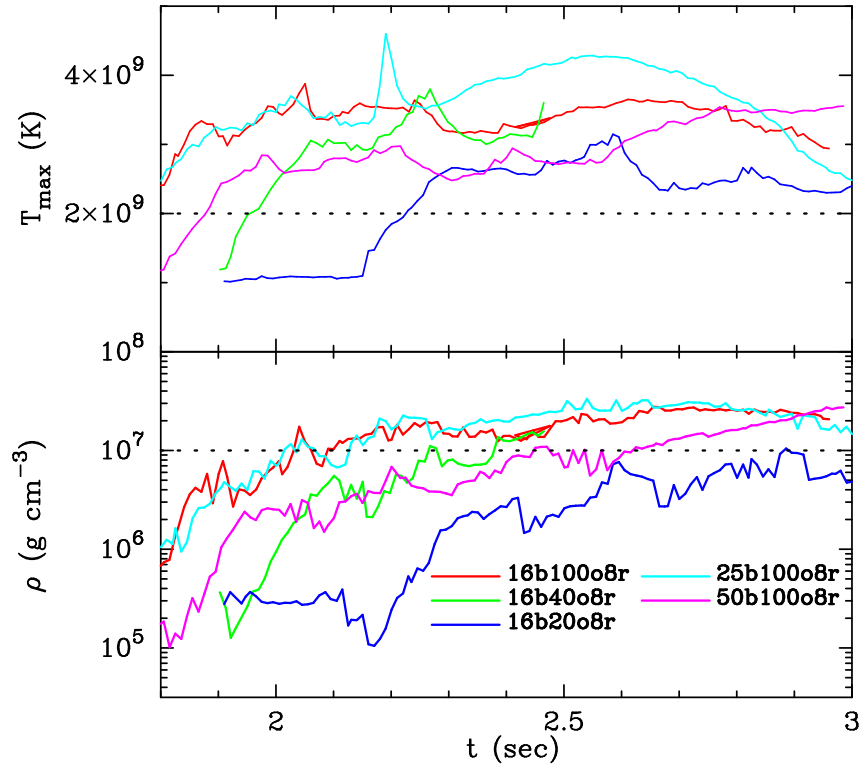


Fig. 2.— Maximum temperature T_{\max} and associated density in the fully refined truncated cone around the “south pole” of the star as a function of time for the five 8km resolution 3-D simulations we performed. The material flowing over the surface of the star enters the lower hemisphere at ~ 1.5 s and collides at ~ 2 s, at which point an inward-directed jet forms. Subsequently, the hot ($T > 3 \times 10^9$ K) material in the jet impacts the surface of the star and becomes compressed, reaching densities $\rho > 1 \times 10^7$ g cm $^{-3}$ in all five of the simulations.

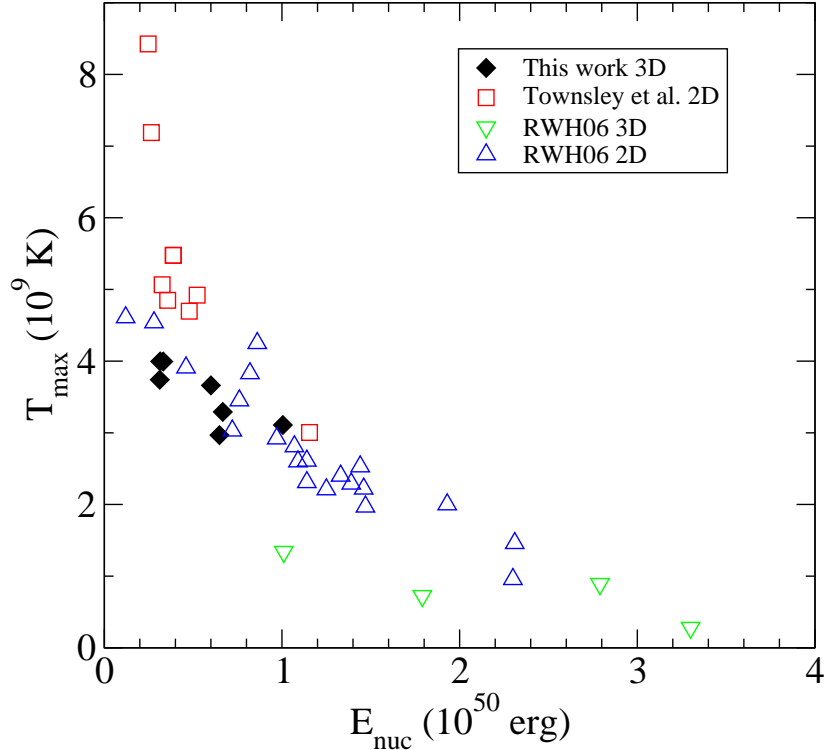


Fig. 3.— Locations in the $(E_{\text{nuc}}, T_{\text{max}})$ -plane of our 2-D and 3-D simulations of the GCD mechanism and of Röpke et al.’s 2-D and 3-D simulations. The seven filled diamonds are (from left to right) for our 16b100o8r, 25b100o6r, 25b100o8r (whose symbols overlap), 16b40o8r, 50b100o8r, 18b42o6r, and 16b20o8r simulations. Note the correlation between E_{nuc} and T_{max} reported by Röpke, Woosley, & Hillebrandt (2007). Our 2-D cylindrical and 3-D simulations both show a relation fairly consistent with Röpke et al.’s 2-D cylindrical simulations, while Röpke et al.’s 3-D simulations disagree with all of these.